Strangeness in a chemically equilibrating quark-gluon plasma

Z. J. He,[1,2,3] J. L. Long,[1] Y. G. Ma,[1,2] G. L. Ma,[1] and B. Liu[4]
[1]*Shanghai Institute of Applied Physics, Chinese Academy of Sciences, P.O. Box 800-204, Shanghai 201800*
[2]*CCAST (World Laboratory), P.O. Box 8730, Beijing 100080, China*
[3]*Research Center of Nuclear Theory of National Laboratory of Heavy Ion Accelerator, Institute of Modern Physics, Chinese Academy of Sciences, Lanzhou 730000, China*
[4]*Institute of High Energy Physics, Chinese Academy of Sciences, Beijing 100039, China*
(Received 27 November 2003; published 22 March 2004)

We derive a set of relaxation equations describing the chemical equilibration of gluons, quarks, and *s* quarks at finite baryon density based on Jüttner distribution of partons, and investigate strangeness production, chemical equilibration, and evolution. We find that strangeness production depends sensitively on initial values, furthermore, the increase of the quark phase lifetime with increasing initial quark chemical potential obviously heightens strangeness production. In addition, the obvious difference between the calculated strangeness and the one in the thermodynamic equilibrium system shows that the study of strangeness in the chemically equilibrating system is very significant.

DOI: 10.1103/PhysRevC.69.034906 PACS number(s): 12.38.Mh, 25.75.−q, 24.85.+p

I. INTRODUCTION

Many experiments are now underway at the Relativistic Heavy-Ion Collider (RHIC) at Brookhaven to study nuclear collisions at very high energies. The hope is to produce a deconfined quark-gluon plasma (QGP). Since QGP exists only for a very short time (several fm) in a small volume (about 100 fm^3), a direct detection of this state of matter is not possible. Thus various indirect signatures have to be used for its detection, such as J/ψ suppression [1], strangeness enhancement [2], dilepton spectra [3–5], etc.

In recent years, Shuryak and co-workers [6,7] have indicated that the QGP produced at RHIC energies may attain kinetic equilibrium but be away from the chemical equilibrium. From master equations governing the evolution of parton densities and equation of energy-momentum conservation of the QGP, Geiger and co-workers [8–11] have studied the dilepton production in baryon-free QGP, and Levai and co-workers [12] have discussed the open charm production. One can note that Hammon and co-workers [13,14] have indicated that the initial system produced at RHIC energies has finite baryon density, Majumder and Gale [15] have discussed the dileptons from QGP at finite baryon density, created at RHIC energies, and recently, Bass *et al.* [16] have pointed out that parton rescattering and fragmentation lead to a substantial increase in the net-baryon density at midrapidity over the density produced by initial primary parton-parton scatterings. These show that one may further study the effect of the chemical equilibration on signatures of the formation of the QGP at finite baryon density. As pointed out in Refs. [10–12,17,18], the distribution functions of partons in a chemically equilibrating system can be described by Jüttner distributions $f_{q(\bar{q})}=\lambda_{q(\bar{q})}/(e^{(p\mp\mu_q)/T}+\lambda_{q(\bar{q})})$ for quarks (antiquarks) and $f_g(p)=\lambda_g/(e^{p/T}-\lambda_g)$ for gluons. When the parton fugacities λ_i are much less than unity as may happen during the early evolution of the parton system, the quantum effect may be neglected, the distributions are approximated as Boltzmann form [19]. However, this introduces larger error when the distribution approaches chemical equilibrium as discussed in Ref. [10]. The most commonly used approximations are the factorized Fermi-Dirac distribution functions $f_{q(\bar{q})}=\lambda_{q(\bar{q})}/(e^{(p\mp\mu_q)/T}+1)$ for quarks (antiquarks) and factorized Bose-Einstein distribution function $f_g(p)=\lambda_g/(e^{p/T}-1)$ for gluons. As can be seen from the discussion in Ref. [10] this approximation coincides with the Jüttner distribution only near $\lambda_g=1$, however, in the intermediate region of the λ_g the deviation is quite significant. It shows that it is difficult to study the whole process of the chemical equilibration of the system based on those previous approximation distribution functions of partons.

At the SPS energies, an enhanced production of strangeness, considered as one of the more robust signatures of the quark-hadron phase transition, has been observed [20–23]. One naturally wonders how strangeness is produced, evolves and depends on finite baryon density in a chemically equilibrating QGP system created at RHIC energies. In order to answer these questions, we should study strangeness of a chemically equilibrating QGP at finite baryon density on the basis of Jüttner distribution of partons, and consider chemical reactions $gg \rightleftharpoons ggg$, $gg \rightleftharpoons q\bar{q}$, $gg \rightleftharpoons s\bar{s}$, and $q\bar{q} \rightleftharpoons s\bar{s}$ in the system. To understand the effect of initial conditions on strangeness, we adopt initial conditions from not only Hijing model calculation [10] but also the self-screened parton cascade (SSPC) model [24]. It is worth emphasizing here the difference between our treatment and that of Ref. [25]. Pal and co-workers [25] have taken the distribution function of partons as $f_j(E_j,\lambda_j)=\lambda_j f_j^{eq}(E_j)$, where $f_j^{eq}(E_j)$ is the thermodynamic equilibrium Bose-Einstein (Fermi-Dirac) distribution for gluons (quarks), and have not considered the effect of the quark chemical potential on strangeness production. Indeed, $f_j(E_j,\lambda_j)$ adopted by them is just the most commonly used approximations as mentioned above. We also indicate that Kapusta and co-workers [26] have studied the *s* quark production in the thermodynamic equilibrium QGP system. In the present work, we shall compare our results with those given in Ref. [26], and discuss the relation between our ap-

proach and that in Ref. [26]. By the way, we note that in a thermodynamic equilibrium QGP system strangeness production has also been studied on the basis of the relativistic hydrodynamic model [27].

The rest of the paper is organized as follows: Section II describes the thermodynamic relations and evolution equations of the system. In Sec. III we discuss the numerical results of strangeness production and evolution. A summary is given in Sec. IV.

II. EVOLUTION OF THE SYSTEM

A. Thermodynamic relations of the system

Considering the chemical potential of s quarks $\mu_s=0$ since s quarks are created in pairs only, we first derive the thermodynamic relations of the chemically equilibrating system at finite baryon density. Expanding densities of quarks (antiquarks) over quark chemical potential μ_q, we get the baryon density of the system [28],

$$n_{b,q}=\frac{g_q}{6\pi^2}\Bigg[T^3(Q_1^2\lambda_q-\overline{Q}_1^2\lambda_{\bar{q}})+2\mu_qT^2(Q_1^1\lambda_q+\overline{Q}_1^1\lambda_{\bar{q}})+T\mu_q^2(Q_1^0\lambda_q-\overline{Q}_1^0\lambda_{\bar{q}})+\frac{1}{3}\mu_q^3\left(\frac{\lambda_q}{\lambda_q+1}+\frac{\lambda_{\bar{q}}}{\lambda_{\bar{q}}+1}\right)\Bigg] \tag{1}$$

and corresponding energy density including contribution from s quarks,

$$\varepsilon_{qgp}=\frac{g_q}{2\pi^2}\Bigg[T^4\left(Q_1^3\lambda_q+\overline{Q}_1^3\lambda_{\bar{q}}+\frac{g_g}{g_q}G_1^3\lambda_g+2\frac{g_s}{g_q}S_1^3\lambda_s\right)+3\mu_qT^3(Q_1^2\lambda_q-\overline{Q}_1^2\lambda_{\bar{q}})+3\mu_q^2T^2(Q_1^1\lambda_q+\overline{Q}_1^1\lambda_{\bar{q}})+T\mu_q^3(Q_1^0\lambda_q-\overline{Q}_1^0\lambda_{\bar{q}})+\frac{1}{3}\mu_q^4\left(\frac{\lambda_q}{\lambda_q+1}+\frac{\lambda_{\bar{q}}}{\lambda_{\bar{q}}+1}\right)+\frac{2\pi^2B_0}{g_q}\Bigg]. \tag{2}$$

We find that taking $\lambda_q=\lambda_{\bar{q}}=\lambda_q=\lambda_s=1$ these equations become the equations of state of the thermodynamic equilibrium QGP system with finite baryon density [18,29], where $g_{q(\bar{q})}$, g_g, and g_s are, in turn, degeneracy factors of quarks (antiquarks), gluons, and s quarks. The integral factors appearing in the expansion above,

$$G_m^n=\int\frac{Z^ndZ}{(e^Z-\lambda_q)^m},\quad Q_m^n(\overline{Q}_m^n)=\int\frac{Z^ndZ}{(\lambda_{q(\bar{q})}+e^Z)^m}, \tag{3}$$

$$S_m^n=\int\frac{Z^ndZ}{(\lambda_s+e^{Z_s})^m},$$

with $Z=p/T$ and $Z_s=[Z^2+(m_s/T)^2]^{1/2}$ are easily calculated, numerically, where m_s is the mass of the s quark. In this work, we consider an ideal fluid, $3P=\varepsilon_{qgp}$, where P is the pressure of the system.

B. Evolution equation of the system

To study strangeness production, we consider the reactions leading to chemical equilibrium not only $gg\rightleftharpoons ggg$ and $gg\rightleftharpoons q\bar{q}$ but also $gg\rightleftharpoons s\bar{s}$ and $q\bar{q}\rightleftharpoons s\bar{s}$. Assuming that elastic parton scatterings are sufficiently rapid to maintain local thermal equilibrium, the evolutions of gluon, quark, and s quark density can be given by the following master equations, respectively,

$$\partial_\mu(n_gu^\mu)=R_3n_g\left[1-\frac{n_g}{\overline{n}_g}\right]-2R_2^{g-q}n_g\left[1-\left(\frac{\overline{n}_g}{n_g}\right)^2\frac{n_q\overline{n}_{\bar{q}}}{\overline{n}_q\overline{n}_{\bar{q}}}\right]-2R_2^{g-s}n_g\left[1-\left(\frac{\overline{n}_g}{n_g}\right)^2\frac{n_s\overline{n}_{\bar{s}}}{\overline{n}_s\overline{n}_{\bar{s}}}\right], \tag{4}$$

$$\partial_\mu(n_qu^\mu)=R_2^{g-q}n_g\left[1-\left(\frac{\overline{n}_g}{n_g}\right)^2\frac{n_q\overline{n}_{\bar{q}}}{\overline{n}_q\overline{n}_{\bar{q}}}\right]-2R_2^{q-s}n_q\left[1-\left(\frac{\overline{n}_q}{n_q}\right)^2\frac{n_s\overline{n}_{\bar{s}}}{\overline{n}_s\overline{n}_{\bar{s}}}\right], \tag{5}$$

and

$$\partial_\mu(n_su^\mu)=R_2^{g-s}n_g\left[1-\left(\frac{\overline{n}_g}{n_g}\right)^2\frac{n_s\overline{n}_{\bar{s}}}{\overline{n}_s\overline{n}_{\bar{s}}}\right]+R_2^{q-s}n_q\left[1-\left(\frac{\overline{n}_q}{n_q}\right)^2\frac{n_s\overline{n}_{\bar{s}}}{\overline{n}_s\overline{n}_{\bar{s}}}\right]. \tag{6}$$

Since the number of s quarks is very small as compared to gluons and light quarks, we can neglect the back reactions $s\bar{s}\rightarrow gg$, $q\bar{q}$, initially. We also note that taking $\lambda_q=\lambda_{\bar{q}}$ does not change the qualitative property of the evolution of the system because the calculated initial quark chemical potential for $A_u^{197}+A_u^{197}$ collisions at RHIC energies is relatively small (see Sec. III). Combining these master equations with equations of baryon number and energy-momentum conservation,

$$\partial_\mu(n_{b,q}u^\mu)=0, \tag{7}$$

$$\frac{\partial\varepsilon_{qgp}}{\partial\tau}+\frac{\varepsilon_{qgp}+P}{\tau}=0, \tag{8}$$

for the longitudinal scaling expansion of the system, we can get a set of relaxation equations describing evolutions of the temperature T, quark chemical potential μ_q, and fugacities λ_q for quarks, λ_g for gluons, and λ_s for s quarks on the basis of the thermodynamic relations of the system with finite baryon density, as obtained above:

$$\left(\frac{1}{\lambda_g}+\frac{G_2^2}{G_1^2}\right)\dot{\lambda}_g+3\frac{\dot{T}}{T}+\frac{1}{\tau}=R_3\left[1-\frac{G_1^2}{2\xi(3)}\lambda_g\right]-2R_2^{g-q}\left[1-\left(\frac{2\xi(3)}{G_1^2}\right)^2\frac{n_q\bar{n_q}}{\bar{n_q}\bar{n_q}}\frac{1}{\lambda_g{}^2}\right]-2R_2^{g-s}\left[1-\left(\frac{2\xi(3)}{G_1^2}\right)^2\frac{n_s\bar{n_s}}{\bar{n_s}\bar{n_s}}\frac{1}{\lambda_g{}^2}\right], \tag{9}$$

$$\dot{\lambda}_q\left[T^3(Q_1^2-\lambda_qQ_2^2)+2\mu_qT^2(Q_1^1-\lambda_qQ_2^1)+T\mu_q^2(Q_1^0-\lambda_qQ_2^0)+\frac{1}{3}\mu_q^3\frac{1}{(\lambda_q+1)^2}\right]+\dot{T}\lambda_q[3T^2Q_1^2+4\mu_qTQ_1^1+\mu_q^2Q_1^0]+\dot{\mu}_q\lambda_q\left[2T^2Q_1^1+2\mu_qTQ_1^0+\mu_q^2\frac{1}{(\lambda_q+1)}\right]+\frac{n_q^0}{\tau}=n_g^0R_2^{g-q}\left[1-\left(\frac{2\xi(3)}{G_1^2}\right)^2\frac{n_q\bar{n_q}}{\bar{n_q}\bar{n_q}}\frac{1}{\lambda_g{}^2}\right]-2R_2^{q-s}\left[1-\left(\frac{\bar{n_q}}{n_q}\right)^2\frac{n_s\bar{n_s}}{\bar{n_s}\bar{n_s}}\right], \tag{10}$$

$$\dot{\lambda}_sT^3(S_1^2-\lambda_sS_2^2)+\dot{T}\lambda_s(3T^2S_1^2+m_s^2D_2^2)+\frac{n_s^0}{\tau}=n_g^0R_2^{g-s}\left[1-\left(\frac{2\xi(3)}{G_1^2}\right)^2\frac{n_s\bar{n_s}}{\bar{n_s}\bar{n_s}}\frac{1}{\lambda_g{}^2}\right]+n_q^0R_2^{q-s}\left[1-\left(\frac{\bar{n_q}}{n_q}\right)^2\frac{n_s\bar{n_s}}{\bar{n_s}\bar{n_s}}\right], \tag{11}$$

$$\dot{\lambda}_q\left[4\mu_qT^2(Q_1^1-\lambda_qQ_1^1)+\frac{2}{3}\mu_q^3\frac{1}{(\lambda_q+1)^2}\right]+\dot{T}8\mu_qTQ_1^1\lambda_q+\dot{\mu}_q\lambda_q\left[4T^2Q_1^1+2\mu_q^2\frac{1}{(\lambda_q+1)}\right]=-\frac{1}{\tau}\lambda_q\left[4\mu_qT^2Q_1^1+\frac{2}{3}\mu_q^3\frac{1}{\lambda_q+1}\right], \tag{12}$$

$$\dot{\lambda}_g\frac{g_g}{g_q}T^4(G_1^3+\lambda_gG_2^3)+\dot{\lambda}_q\left[2T^4(Q_1^3-\lambda_qQ_2^3)+6T^2\mu_q^2(Q_1^1-\lambda_qQ_2^1)+\frac{2}{4}\mu_q^4\frac{1}{(\lambda_q+1)^2}\right]+\dot{\lambda}_s\frac{2g_s}{g_q}T^4(S_1^3-\lambda_sS_2^3)+\dot{T}\left[8T^3Q_1^3\lambda_q+12\mu_q^2TQ_1^1\lambda_q+4\frac{g_g}{g_q}T^3\lambda_gG_1^3+\frac{2g_s}{g_q}T\lambda_s(4T^2S_1^3+m_s^2D_2^3)\right]+\dot{\mu}_q\lambda_q\left[12\mu_qT^2Q_1^1+2\mu_q^3\frac{1}{\lambda_q+1}\right]=-\frac{1}{\tau}\left[2T^4Q_1^3\lambda_q+6\mu_q^2T^2Q_1^1\lambda_q\left(\frac{\lambda_q}{\lambda_q+1}\right)+\frac{g_g}{g_q}T^4\lambda_gG_1^3+\frac{g_s}{g_q}T^4\lambda_sS_2^3\right], \tag{13}$$

where $\bar{n}_{q(\bar{q})}$ is the value of $n_{q(\bar{q})}$ at $\lambda_{q(\bar{q})}=1$, $n_q^0=n_q/(g_q/2\pi^2)$, $n_g^0=n_g/(g_g/2\pi^2)$, $\xi(3)=1.202\,06$, integral factor $D_m^n=\int dZ\, e^{Z_s}Z^n/[(\lambda_s+e^{Z_s})^mZ_s]$ with $Z_s=[Z^2+(m_s/T)^2]^{1/2}$, and m_s the mass of the s quark, again. Since the chemical potential of s quarks is zero, in baryon number conservation equation (12) the influence from s quarks cannot be seen directly. Adopting factorizations as done in Refs. [10,12], we have production rates for processes $gg\rightarrow ggg$, $gg\rightarrow q\bar{q}$, and $gg\rightarrow s\bar{s}$:

$$R_3=\tfrac{1}{2}\sigma_3n_g,R_2^{g-q}=\tfrac{1}{2}\sigma^{g-q}n_g,$$

$$R_2^{g-s}=\tfrac{1}{2}\sigma^{g-s}n_g, \tag{14}$$

where σ_3, σ^{g-q}, and σ^{g-s} are, in turn, thermally averaged, velocity weighted cross sections,

$$\sigma_3=\langle\sigma(gg\rightarrow ggg)v_{12}\rangle,\quad \sigma^{g-q}=\langle\sigma(gg\rightarrow q\bar{q})v_{12}\rangle,$$

$$\sigma^{g-s}=\langle\sigma(gg\rightarrow ss)v_{12}\rangle, \tag{15}$$

where v_{12} is the relative velocity between the initial particles. Finally, the corresponding production rates R_3/T, R_2^{g-q}/T, and R_2^{g-s}/T are, in turn, given by

$$R_3/T=\frac{32}{3a_1}\frac{\alpha_s}{\lambda_g}\left[\frac{(M_D^2+s/4)M_D^2}{9g^2T^4/2}\right]^2I(\lambda_g,\lambda_q,T,\mu_q), \tag{16}$$

$$R_2^{g-q}/T=\frac{g_g}{24\pi}\frac{G_1^{12}}{G_1^2}N_f\alpha_s^2\lambda_g\ln(1.65/\alpha_s\lambda^{(q)}), \tag{17}$$

$$R_2^{g-s}/T=\frac{g_g}{24\pi}\frac{G_1^{12}}{G_1^2}N_f\alpha_s^2\lambda_g\ln(1.65/\alpha_s\lambda^{(s)}), \tag{18}$$

$$M_D^2 = \frac{3g^2T^2}{\pi^2}\left[2G_1^1\lambda_g + 2N_f Q_1^1\lambda_q + \left(\frac{\mu_q}{T}\right)^2\left(\frac{\lambda_q}{\lambda_q+1}\right)\right] \tag{19}$$

with

$$\lambda^{(q)} = \lambda_g + \frac{1}{G_1^1}\left[Q_1^1\lambda_q + \left(\frac{\mu_q}{T}\right)^2\left(\frac{\lambda_q}{\lambda_q+1}\right)\right], \tag{20}$$

$$\lambda^{(s)} = \lambda_g + \frac{1}{G_1^1}S_1^1\lambda_s, \tag{21}$$

and the QCD running coupling constant α_s is given by

$$\alpha_s(T) = \frac{6\pi}{27\ \ln[T/(50\ \text{MeV})]}. \tag{22}$$

M_D is the Debye screening mass, $s=18T^2$, $a_1=2\pi^2 g_g G_1^2$, $I(\lambda_g,\lambda_q,T,\mu_q)$ the function of λ_g, λ_q, T, μ_q [12], and N_f the quark flavor. Similarly, the production rate R_2^{q-s}/T for process $q\bar{q}\to s\bar{s}$ is calculated via taking cross section $\sigma(q\bar{q}\to s\bar{s})$ from Ref. [30].

III. CALCULATED RESULTS AND DISCUSSIONS

A. Initial values of the system

Hammon and co-workers [13] have calculated nonequilibrium initial conditions from perturbative QCD within the Glauber multiple scattering theory for $\sqrt{s}=200A$ GeV. Considering higher-order contribution by a factor $K=2.5$ from comparison with experiment at the RHIC [31], they have obtained the energy density and number densities of gluons, quarks, and antiquarks as well as the initial temperature $T_0=0.552$ GeV. From these densities we have also obtained initial temperature $T_0=0.566$ GeV and initial quark chemical potential $\mu_{q0}=0.284$ GeV based on thermodynamic relations of the chemically equilibrating system at finite baryon density, as mentioned in Sec. II A, at $\lambda_{g0}=0.09$ and $\lambda_{q0}=0.02$. Obviously, these initial temperatures are near the one from Hijing model calculation, as shown in Ref. [10]. With the help of Ref. [10] we take initial values: $\tau_0=0.70$ fm, $T_0=0.57$ GeV, $\lambda_{g0}=0.09$, $\lambda_{q0}=0.02$, and $\lambda_{s0}=0.01$. To further understand the effect of finite baryon density on strangeness, we extend our calculation up to the initial quark chemical potential $\mu_{q0}=0.568$ GeV. Finally, we have solved the set of relaxation equations (9)–(13) for initial quark chemical potentials $\mu_{q0}=0.000$, 0.284, and 0.568 GeV, and obtained the evolutions of the temperature, quark chemical potential, and fugacities λ_g, λ_q, and λ_s. For comparison, we have also solved the same set of equations for those initial values obtained from the SSPC model [24]: $\tau_0=0.25$ fm, $T_0=0.67$ GeV, $\lambda_{g0}=0.34$, $\lambda_{q0}=0.068$, and $\lambda_{s0}=0.034$.

B. Cooling of the system

The calculated evolution paths of the system in the phase diagram have been shown in Fig. 1, where the dashed, solid, and dotted lines denote, in turn, the calculated paths for initial quark chemical potentials $\mu_{q0}=0.000$, 0.284, and 0.568 GeV at $T_0=0.57$ GeV, $\tau_0=0.70$ fm, $\lambda_{g0}=0.09$, $\lambda_{q0}=0.02$, and $\lambda_{s0}=0.01$, and the dash-dotted line is the phase boundary between the quark phase and the hadronic phase.

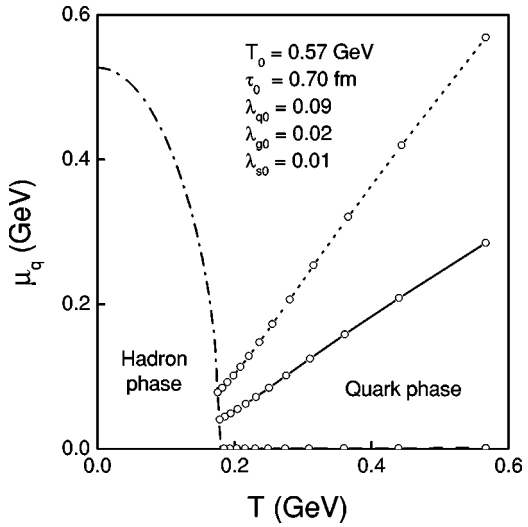

FIG. 1. The bag model phase diagram is calculated at $B^{1/4}=0.25$ GeV. The calculated evolution paths of the system in the phase diagram for initial values $\tau_0=0.70$ fm, $T_0=0.57$ GeV, $\lambda_{g0}=0.09$, $\lambda_{q0}=0.02$, and $\lambda_{s0}=0.01$, where the dashed, solid, dotted lines are, in turn, the evolution paths for initial quark chemical potentials $\mu_{q0}=0.000$, 0.284, and 0.568 GeV, and the dash-dotted line is the phase boundary of the phase diagram. The time interval between the two small circles is 0.3 fm (i.e., $30\times$calculation-step 0.01 fm).

Now, we discuss the effect of the finite initial quark chemical potential on the evolution of the system. One has known that the baryon-free QGP converts into the hadronic matter only with decreasing the temperature along the temperature axis of the phase diagram, and the phase transition occurs at a certain critical temperature T_c. However, in this work, both the quark chemical potential and the temperature of the system are functions of time, compared with the baryon-free QGP it necessarily takes a long time for value (μ_q,T) of the system to reach a certain point of the phase boundary to make the phase transition. Such an effect will cause the increase of the lifetime of the quark phase. Furthermore, we have found that with increasing the initial quark chemical potential, the production rate R_3/T of gluons goes up (see Fig. 2) and the gluon equilibration rate necessarily goes down (see Fig. 3), thus leading to the little energy consumption of the system, i.e., slow cooling of the system. Since gluons are much more than quarks in the system, overall with increasing the initial quark chemical potential, the cooling of the system further slows down. One can see in Fig. 1 that the increase of the initial quark chemical potential will change the hydrodynamic behavior of the system to cause the increase of the quark phase lifetime. The calculated presence times of the system in the quark phase for initial quark chemical potentials $\mu_q=0.000$, 0.284, and 0.568 GeV are, in turn, about 3.57, 3.76, and 3.95 fm. Compared with those values calculated in Ref. [28], one can see that due to inclusion of reactions $gg\to s\bar{s}$ and $q\bar{q}\to s\bar{s}$, the energy consumption of the system becomes even faster. In order to give

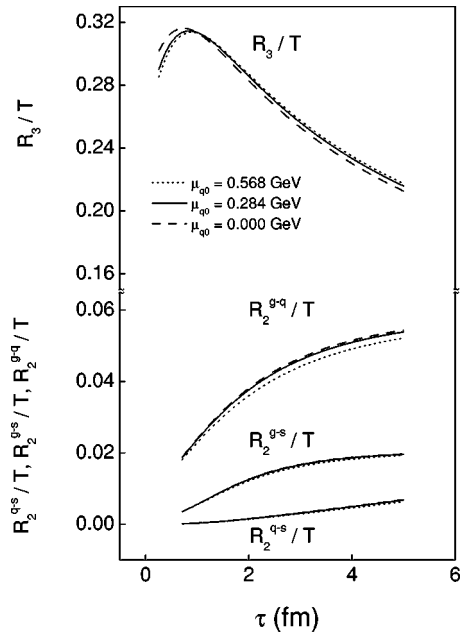

FIG. 2. The calculated parton production rates at the same initial conditions as given in Fig. 1. The gluon, quark, $g \to s$ and $q \to s$ production rates are denoted by R_3/T, R_2^{g-q}/T, R_2^{g-s}/T, and R_2^{q-s}/T, respectively. The dashed, solid, and dotted lines denote, respectively, the production rates for initial quark chemical potentials $\mu_{q0}=0.000$, 0.284, and 0.568 GeV.

a deeper insight into the dynamical evolution of the system, we have marked the equal time step on the paths in Fig. 1. The time interval between the two small circles is 0.30 fm (i.e., $30\times$ calculation-step 0.01 fm). We can clearly see from Fig. 1 that the evolution of the system becomes slower and slower towards reaching the phase boundary.

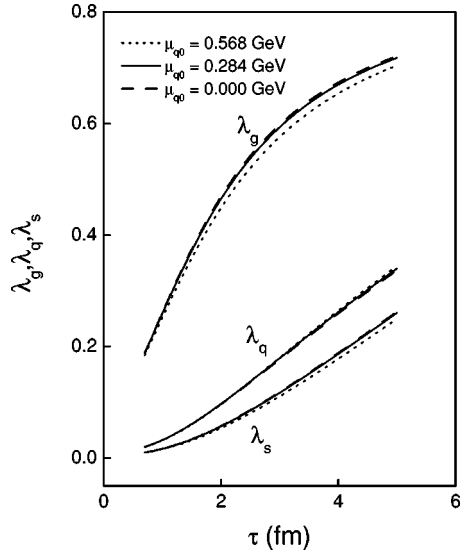

FIG. 3. The calculated equilibration rates at the same initial conditions as given in Figs. 1 and 2. The gluons, quarks, and s quark equilibration rates are, in turn, denoted by λ_g, λ_q, and λ_s. The dashed, solid, and dotted lines denote, respectively, the equilibration rates for initial quark chemical potentials $\mu_{q0}=0.000$, 0.284, and 0.568 GeV.

C. Chemical equilibration of the system

We further discuss the chemical equilibration of the system. The calculated gluon, $g \to q$, $g \to s$, and $q \to s$ production rates R_3/T, R_2^{g-q}/T, R_2^{g-s}/T, and R_2^{q-s}/T are shown in Fig. 2. The corresponding equilibration rates of gluons, quarks and s quarks λ_g, λ_q, and λ_s are shown in Fig. 3. The dashed, solid, and dotted lines in Figs. 2 and 3 denote, respectively, the calculated values for initial quark chemical potentials $\mu_{q0}=0.000$, 0.284, and 0.568 GeV. Due to adopting Jüttner distribution as phase space distribution function of partons, the Debye screening mass M_D^2 rises with the quark chemical potential as seen in Eq. (19). The calculation results show that the quark chemical potential goes down with evolution time, hence according to Eq. (16) the gluon production rate R_3/T will rapidly go down with evolution time as seen in Fig. 2, while the chemical equilibration rate λ_g of gluons necessarily goes up rapidly with evolution time as shown in Fig. 3. Obviously, in order to establish the chemical equilibrium of the system the production rates R_2^{g-q}/T and R_2^{g-s}/T should go up with evolution time, as seen in Fig. 2. The behaviors of these production rates are mainly governed by the gluon production (or chemical equilibration), accordingly, the gluon equilibration rate λ_g is included in Eqs. (17) and (18). For the same reason, the rate R_2^{q-s}/T should also rise with evolution time.

In order to understand the influence of initial values on the chemical equilibration of the system, we have calculated the chemical equilibration rate of s quarks for initial values $\lambda_{g0}=\lambda_{q0}=1$ (i.e., in a chemically equilibrated QGP system) and $\mu_{q0}=0.284$ GeV. The calculated result is shown by the dash-dotted line in Fig. 4, while the solid line is taken from Fig. 3, which is calculated at initial values $\lambda_{g0}=0.09$, $\lambda_{q0}=0.02$, and $\mu_q=0.284$ GeV. The set of relaxation equations (9)–(13) governs the system to tend to the chemical equilibrium, i.e., $\lambda_g=\lambda_q=\lambda_s=1$. After quarks and gluons reach the chemical equilibrium, only few quarks and gluons can join chemical reactions during the evolution, thus, equilibration rates λ_g and λ_q have to adopt the evolution ways as shown by the dot-dot-dashed line and dotted line in Fig. 4, respectively. Accordingly the s quark production rate necessarily goes down and chemical equilibration rate goes up, rapidly. Thus, we can see that in Fig. 4 λ_s shown by the dash-dotted line rises much more rapidly with increasing the evolution time than the one shown by the solid line. It shows that the chemical equilibration of strangeness depends sensitively on the initial value.

D. Strangeness production of the system

We have calculated strangeness $n_s/\overline{n_s}$ according to the relation

$$n_s = \frac{g_s T^3}{2\pi^2} \int \frac{\lambda_s Z^2 dZ}{e^{[Z^2 + (m_s/T)^2]^{1/2}} + \lambda_s} \tag{23}$$

from the calculated s quark equilibration rate λ_s and temperature T as well as s quark mass m_s, where $\overline{n_s}$ is the value of n_s at $\lambda_s=1$, and $Z=p/T$ again. In Fig. 5, the dotted and solid lines are, in turn, the calculated strangeness for the two

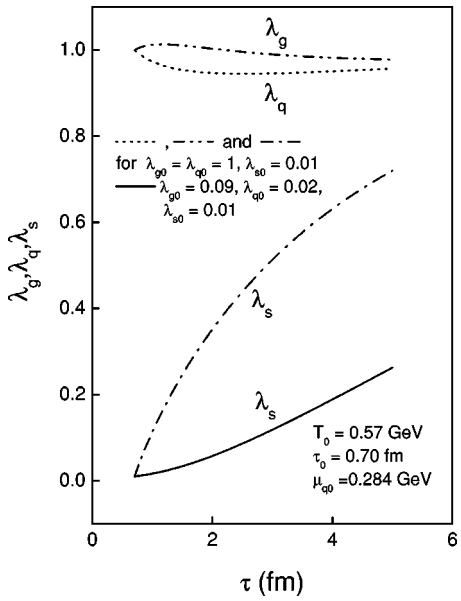

FIG. 4. The calculated chemical equilibration rate of *s* quarks in the quark and gluon chemically equilibrated system (i.e., $\lambda_{g0}=\lambda_{q0}=1$) for initial values $\tau_0=0.7$ fm, $T_0=0.57$ GeV, $\mu_{s0}=0.284$ GeV, and $\lambda_{s0}=0.01$. The dash-dotted, dotted, and dot-dot-dashed lines are, in turn, the calculated equilibration rates λ_s, λ_q, and λ_g, while the solid line is the *s* quark equilibration rate, for $\mu_{s0}=0.284$ GeV, taken from Fig. 3.

sets of initial values: $\tau_0=0.70$ fm, $T_0=0.57$ GeV, $\lambda_{g0}=0.09$, $\lambda_{q0}=0.02$, and $\lambda_{s0}=0.01$; $\tau_0=1.00$ fm, $T_0=0.57$ GeV, $\lambda_{g0}=\lambda_{q0}=1$, and $\lambda_{s0}=0.01$ as used above. Since at initial values $\lambda_{g0}=\lambda_{q0}=1$ the equilibration rate λ_s goes up even more rapidly with evolution time, as seen in Fig. 4, moreover, Eq. (23) shows that strangeness is directly proportional to the equilibration rate λ_s, one can see that the solid line

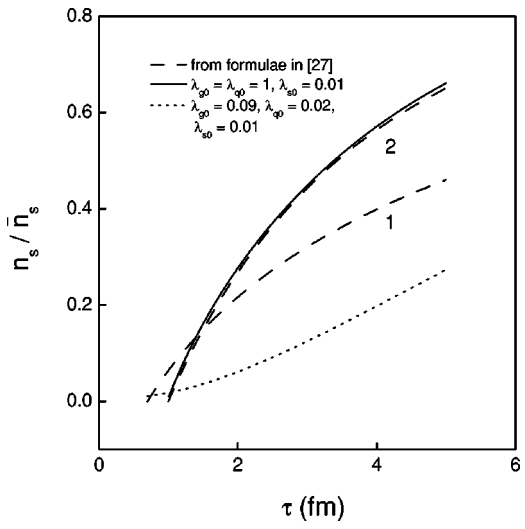

FIG. 5. The calculated strangeness $n_s/\bar{n_s}$. The dotted and solid lines are, in turn, the calculated values for the same initial values as given in Figs. 1–3 at $\tau_0=0.70$ fm, and for initial values $\lambda_{g0}=\lambda_{q0}=1.00$, and $\lambda_{s0}=0.01$ at $\tau_0=1.00$ fm. The dashed lines 1 and 2 are the calculated values in the thermodynamic equilibrium system [26] for initial values $\tau_0=0.7$ and 1.0 fm at $n_s(\tau_0)=0$, respectively.

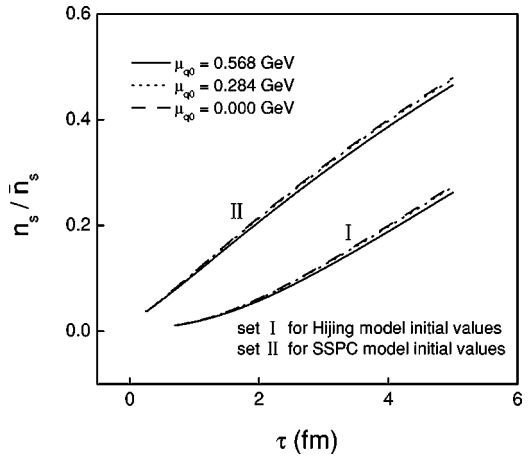

FIG. 6. The calculated strangeness $n_s/\bar{n_s}$. The set I of lines and set II of lines are, respectively, obtained from initial values given by the Hijing model as seen in Fig. 1, and from that given by SSPC model ($T_0=0.67$ GeV, $\tau_0=0.25$ fm, $\lambda_{g0}=0.34$, $\lambda_{q0}=0.068$, and $\lambda_{s0}=0.034$). The dashed, dotted, and solid lines denote, in turn, those calculated values for initial quark chemical potentials $\mu_{q0}=0.000$, 0.284, and 0.568 GeV.

rises much more rapidly than the dotted line in Fig. 5. The dashed lines 1 and 2 are obtained in the thermodynamic equilibrium QGP system as described in Ref. [26] at $\tau_0=0.7$ and 1.0 fm for $n_s(\tau_0)=0$, respectively. One can note that in Fig. 5 the solid line coincides with the dashed line 2 in the region we are interested in. It shows that strangeness evolution in the system at initial values $\tau_0=1.00$ fm, $T_0=0.57$ GeV, $\lambda_{g0}=\lambda_{q0}=1$, and $\lambda_{s0}=0.01$ is almost the same as the one obtained in the thermodynamic equilibrium system [26] at $\tau_0=1.0$ fm, $T_0=0.57$ GeV, and $n_s(\tau_0)=0$. Obviously the present framework can also approach strangeness evolution of the thermodynamic equilibrium system. Furthermore, we find in Fig. 5 that strangeness evolution in the chemically equilibrating system is very different from the one in the chemically equilibrated system. It shows that it is very significant to study strangeness in the chemically equilibrating QGP.

In Fig. 6 the first set of lines and second set of lines are obtained at initial values from the Hijing model [10] and SSPC model [24], respectively. The dashed, dotted, and solid lines denote, in turn, the calculated strangeness for initial quark chemical potentials $\mu_{q0}=0.000$, 0.284, and 0.568 GeV. As pointed out in Sec. III B, the cooling of the system slows down with increasing the initial quark chemical potential, accordingly one should see that strangeness goes up with the increase of the initial quark chemical potential. However, because of inclusion of reactions $gg\rightarrow s\bar{s}$ and $q\bar{q}\rightarrow s\bar{s}$, the cooling of the system becomes even faster, as pointed out above, on the other hand strangeness is only indirectly affected by the quark chemical potential through the effect of the quark chemical potential on the temperature, in particular, owing to adopting strangeness expression $n_s/\bar{n_s}$, factor T^3 in n_s and $\bar{n_s}$ is canceled, thus, the effect of the quark chemical potential on strangeness is only given through the *s* quark chemical equilibration rate λ_s and temperature T included in denominator of Eq. (23). Since with increasing the

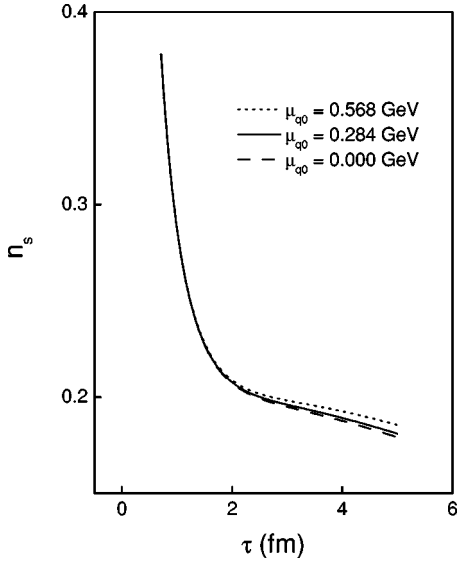

FIG. 7. The calculated strangeness n_s for initial values $\tau_0 = 0.70$ fm, $T_0 = 0.57$ GeV, $\lambda_{g0} = 0.09$, $\lambda_{q0} = 0.02$, and $\lambda_{s0} = 0.01$. The dashed, solid, and dotted lines denote, respectively, the calculated values for initial chemical potentials $\mu_{q0} = 0.000$, 0.284, and 0.568 GeV.

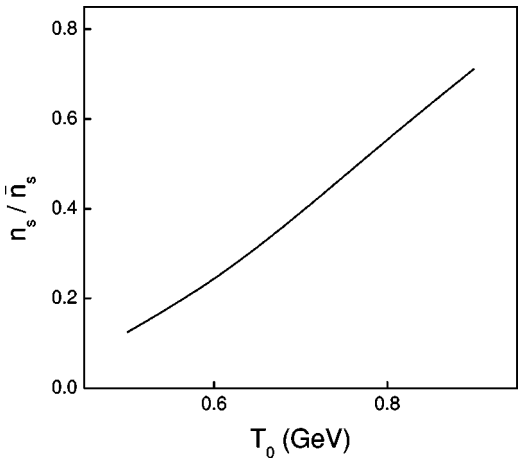

FIG. 8. The calculated strangeness at the phase boundary as a function of the initial temperature T_0 for initial conditions $\tau_0 = 0.70$ fm, $\lambda_{g0} = 0.09$, $\lambda_{q0} = 0.02$, $\lambda_{s0} = 0.01$, and $\mu_{q0} = 0.284$ GeV.

quark chemical potential λ_s goes down as indicated above, strangeness necessarily goes down with the initial quark chemical potential, as shown in Fig. 6. In addition, comparing the two sets of lines in Fig. 6, one can note that the calculated strangeness under initial values from the SSPC model is larger than the one under initial values from the Hijing model since the initial temperature from the SSPC model is higher than the one from the Hijing model.

In order to further understand the relation between the initial quark chemical potential μ_{q0} and strangeness production in the chemically equilibrating QGP, we have calculated strangeness n_s for initial values $\tau_0 = 0.70$ fm, $T_0 = 0.57$ GeV, $\lambda_{g0} = 0.09$, $\lambda_{q0} = 0.02$, and $\lambda_{s0} = 0.01$, as shown in Fig. 7, where the dashed, solid, and dotted lines denote, respectively, the calculated values for initial quark chemical potentials $\mu_{q0} = 0.000$, 0.284, and 0.568 GeV. Since the effect of the initial quark chemical potential on strangeness is more completely included in the calculation through the temperature T and s quark equilibration rate λ_s, the calculated strangeness rises more obviously with increasing the initial quark chemical potential. In Eq. (23), s quark equilibration rate λ_s goes up with evolution time as seen in Fig. 3, while the rest part of the equation goes down, thus making turning points in Fig. 7, which signal that the QGP is a chemically equilibrating system.

Finally, the calculated strangeness at the phase boundary for initial conditions $\tau_0 = 0.70$ fm, $\lambda_{g0} = 0.09$, $\lambda_{q0} = 0.02$, $\lambda_{s0} = 0.01$, and $\mu_{q0} = 0.284$ GeV as a function of the initial temperature T_0 is shown in Fig. 8. One can see that the curve goes up approximately linearly with the initial temperature T_0 in the region from the temperature (about 0.60 GeV) of the RHIC to the one (about 0.90 GeV) of the LHC [12].

IV. SUMMARY

In order to study strangeness production in a chemically equilibrating QGP system at finite baryon density, we have included the dominant reactions leading to chemical equilibrium $gg \rightleftharpoons ggg$, $gg \rightleftharpoons q\bar{q}$, $gg \rightleftharpoons s\bar{s}$, and $q\bar{q} \rightleftharpoons s\bar{s}$ in the system. Then, based on the Jüttner distribution of partons for the Bjorken longitudinal scaling expansion from conservation laws of the energy momentum and baryon number of the system, we have derived a set of relaxation equations governing evolutions of the temperature T, quark chemical potential μ_q, and fugacities λ_q for quarks, λ_g for gluons, and λ_s for s quarks. Subsequently, we have solved the set of relaxation equations, and studied strangeness production. The calculation results show that the gluon production rate goes down and s quark and quark production rates go up with evolution time. It shows that the present framework reasonably describes parton evolution ($gg \rightarrow ggg$, $gg \rightarrow q\bar{q}$, $gg \rightarrow s\bar{s}$, and $q\bar{q} \rightarrow s\bar{s}$) in the system. From calculated production rates (see Fig. 2) we have seen that s quarks are mostly produced in the evolution stage of the system with the temperature of more than about 300 MeV ($\sim 2m_s$) for a very short time from τ_0 (0.70 fm) to about 2.0 fm, and the QGP system does not attain chemical equilibrium by the time it reaches the phase boundary. We have also found that when taking the initial values $\tau_0 = 1.0$ fm, $T_0 = 0.57$ GeV, and $\lambda_{g0} = \lambda_{q0} = 1$, the calculated strangeness coincides almost with the one obtained in the thermodynamic equilibrium QGP system at $\tau_0 = 1.0$ fm, $T_0 = 0.57$ GeV, and $n_s(\tau_0) = 0$. It shows that the present framework may also qualitatively approach strangeness production in the thermodynamic equilibrium QGP system. Especially, the calculated strangeness in the chemically equilibrating system is very different from the one calculated in the thermodynamic equilibrium QGP system. It shows that it is very significant to study strangeness in the chemically equilibrating QGP and may help us look for signatures of the QGP formation and explore the thermodynamic properties of the QGP. We have also noted that the increase of the initial quark chemical potential will change the hydrodynamic behavior of the chemically equilibrating QGP system to cause the increase of the quark phase lifetime. This effect will heighten strangeness production. Even if due to inclusion of reactions $gg \rightarrow s\bar{s}$ and $q\bar{q} \rightarrow s\bar{s}$, the cooling rate of the system somewhat rises, strangeness production is only indirectly af-

fected by the quark chemical potential through the temperature and *s* quark chemical equilibration rate λ_s, as well as the evaluated quark chemical potential ($\sim$0.284 GeV) at RHIC energies is not large, the effect of the quark chemical potential can still more obviously heighten strangeness n_s. However, we stress that the strangeness equilibrium ratio $n_s/\overline{n_s}$ goes down by increasing the initial quark chemical potential since factors T^3 cancel in n_s and $\overline{n_s}$. Obviously, in order to understand the relation between the strangeness production and other physical factors, it is useful to consider the produced strangeness density n_s instead of the ratio $n_s/\overline{n_s}$. In addition, we find that the ratio $n_s/\overline{n_s}$ at the phase boundary approximately linearly depends on the initial temperature. This implies that the relation between strange particle production and the initial temperature remains simple, if the phase transition is fast, and leads to an immediate hadronization and breakup without a hadronic after-burner stage, as it is suggested by several hadronization models based on quark coalescence [32–34].

In this work, we have studied strangeness production in a chemically equilibrating QGP system at finite baryon density for the Bjorken longitudinal scaling expansion model, neglected the effect of the nonhomogeneous distribution of the particle in space, higher-order gluon processes, and back reactions $s\overline{s}\rightarrow gg$, $q\overline{q}$. In the calculation, we have taken $m_s = 0.15$ GeV and $K = 2.5$ to include contribution from next-to-leading order.

ACKNOWLEDGMENTS

This work was supported in part by CAS knowledge Innovation Project No. KJCX2-N11, the National Natural Science Foundation of China under Grant Nos. 10075071, 10275002, 10328509, and 10135030, the Major State Basic Research Development Program in China under Contract No. G200077400.

[1] T. Matsui and H. Satz, Phys. Lett. B **178**, 416 (1986).
[2] J. Rafelski and B. Müller, Phys. Rev. Lett. **48**, 1066 (1982).
[3] E. Shuryak, Phys. Rep. **80**, 71 (1980).
[4] K. Kajantie, J. Kapusta, L. McLerran, and A. Mekjian, Phys. Rev. D **34**, 2746 (1986).
[5] A. Dumitru *et al.*, Phys. Rev. Lett. **70**, 2860 (1993).
[6] E. Shuryak, Phys. Rev. Lett. **68**, 3270 (1992).
[7] K. J. Eskola and X. N. Wang, Phys. Rev. D **49**, 1284 (1994).
[8] K. Geiger, Phys. Rev. D **48**, 4129 (1993).
[9] E. Shuryak and L. Xiong, Phys. Rev. Lett. **70**, 2241 (1993).
[10] T. S. Biró *et al.*, Phys. Rev. C **48**, 1275 (1993).
[11] C. T. Traxler and M. H. Thoma, Phys. Rev. C **53**, 1348 (1996).
[12] P. Levai, B. Müller, and X. N. Wang, Phys. Rev. C **51**, 3326 (1995).
[13] N. Hammon, H. Stöcker, and W. Greiner, Phys. Rev. C **61**, 014901 (1999).
[14] K. Geiger and J. I. Kapusta, Phys. Rev. D **47**, 4905 (1993).
[15] A. Majumder and C. Gale, Phys. Rev. D **63**, 114008 (2001).
[16] S. A. Bass, B. Müller, and D. K. Srivastava, Phys. Rev. Lett. **91**, 052302 (2003).
[17] T. Matsui, B. Svetitsky, and L. D. McLerran, Phys. Rev. D **34**, 783 (1986).
[18] B. Kämpfer *et al.*, Z. Phys. A **353**, 71 (1995).
[19] B. Kämpfer, O. P. Pavlenko, A. Peshier, and G. Soff, Phys. Rev. C **52**, 2704 (1995).
[20] M. Gyulassy, Nucl. Phys. **A418**, 594c (1984).
[21] T. Matsui, B. Svetitsky, and L. D. McLerran, Phys. Rev. D **34**, 783 (1986).
[22] K. Geiger, Phys. Rev. D **48**, 4129 (1993).
[23] J. Letessier and J. Rafelski, Nucl. Phys. **A661**, 497c (2000).
[24] K. J. Eskola, B. Müller, and X. N. Wang, Phys. Lett. B **374**, 20 (1996).
[25] D. Pal, A. Sen, M. G. Mustafa, and D. K. Srivastava, Phys. Rev. C **65**, 034901 (2002).
[26] J. Kapusta and A. Mekjian, Phys. Rev. D **33**, 1304 (1986).
[27] Z. J. He, J. J. Zhang, and B. S. Zhou, J. Phys. G **19**, L7 (1993).
[28] Z. He, J. Long, W. Jiang, Y. Ma, and B. Liu, Phys. Rev. C **68**, 024902 (2003).
[29] L. H. Xia, C. M. Ko, and C. T. Li, Phys. Rev. C **41**, 572 (1990).
[30] B. L. Combridge, Nucl. Phys. **B151**, 429 (1979).
[31] K. J. Eskola, K. Kajantie, and J. Lindfors, Nucl. Phys. **B323**, 37 (1989); C. Albaja *et al.*, UA1 Collaboration, *ibid.* **B309**, 405 (1988).
[32] V. Greco, C. M. Ko, and P. Lévai, Phys. Rev. Lett. **90**, 202302 (2003).
[33] R. J. Fries, B. Müller, C. Nonaka, and S. A. Bass, Phys. Rev. Lett. **90**, 202303 (2003).
[34] R. C. Hwa and C. B. Yang, Phys. Rev. C **67**, 034902 (2003).